Article

Modern Urban Living; Air Quality in Two Northern Greek Cities

Maria-Elissavet Koukouli[1*], Andreas Pseftogkas[1], Dimitris Karagkiozidis[1], Ioanna Skoulidou[1], Theano Drosoglou[1], Dimitrios Balis[1], Alkiviadis Bais[1], Dimitrios Melas[1] and Nikos Hatzianastassiou[2]

[1] Laboratory of Atmospheric Physics, Aristotle University of Thessaloniki, Thessaloniki, Greece; mariliza@auth.gr (M.-E. K.); anpsefto@auth.gr (A. P.); dkaragki@auth.gr (D.K.); ioannans@auth.gr (I. S.); tdroso@noa.gr (T. D.); balis@auth.gr (D. B.); abais@auth.gr (A. B.); melas@auth.gr (D. M.)
[2] Laboratory of Meteorology, Department of Physics, University of Ioannina, Ioannina, Greece; nhatzian@uoi.gr (N. H.)
* Correspondence: mariliza@auth.gr

Abstract: In this article, we aim to show the capabilities, benefits, as well as restrictions, of three different air quality-related information sources, namely the Sentinel-5Precursor TROPOspheric Monitoring Instrument (TROPOMI) space-born observations, the Multi-Axis Differential Optical Absorption Spectroscopy (MAX-DOAS) ground-based measurements and the LOng Term Ozone Simulation – EURopean Operational Smog (LOTOS-EUROS) chemical transport modelling system simulations. The tropospheric NO_2 concentrations between 2018 and 2021 are discussed as air quality indicators for the Greek cities of Thessaloniki and Ioannina. Each dataset was analysed in an autonomous manner and, without disregarding their differences, the common air quality picture that they provide is revealed. All three systems report a clear seasonal pattern, with high NO_2 levels during winter-time and lower NO_2 levels during summer-time, reflecting the importance of photochemistry in the abatement of this air pollutant. The spatial patterns of the NO_2 load, obtained by both space-born observations and model simulations, show the undeniable variability of the NO_2 load within the urban agglomerations. Furthermore, a clear diurnal variability is clearly identified by the ground-based measurements, as well as a Sunday minimum NO_2 load effect, alongside the rest of the sources of air quality information. Within their individual strengths and limitations, the space-born observations, the ground-based measurements, and the chemical transport modelling simulations, demonstrate unequivocally their ability to report on the air quality situation in urban locations.

Keywords: remote sensing; air quality; NOx emissions; S5P/TROPOMI; MAX-DOAS; LOTOS-EUROS

1. Introduction

In recent decades, with the ever increasing urbanisation and human need for modern living conditions, air quality has become a major concern affecting billions of people globally. According to the World Health Organization, WHO, in 2016, 91% of the world population was exposed to conditions where the WHO air quality guidelines levels were not met (WHO, 2016) while ambient air pollution, both in urban and rural areas, was estimated to cause 4.2 million premature deaths worldwide. For Greece and year 2015, the European Environment Agency, (EEA, 2018) estimated that about 12000 premature deaths were attributable to particulate matter (PM2.5 & PM10) concentrations, over 6100 to ozone (O_3), concentrations and 2300 to nitrogen dioxide (NO_2) concentrations. Monitoring of air quality is traditionally performed by ground-based *in situ* stations and the European Environmental Agency, EEA, is basing its annual assessments of the status, impact and recent air quality trends on measurements at fixed sampling stations (EEA, 2020.) The EU

 doi:10.20944/preprints202204.0257.v1

Environmental Implementation Review 2019 for Greece (EU, 2019), reports that exceedances related to the annual limit value for NO_2 were registered in 1 out of 4 air quality zones (the capital city of Athens), in 1 out of 4 zones for PM2.5 and in 3 out of 4 zones for PM10. These official statistics are however relying on the network of in situ air quality stations reporting to the EEA Air Quality Data Service, (EEA, 2022), which are rarely indicative of the true situation; in Greece, only four cities are represented in this database, with no indication on the status over the rest of the mainland, the islands and background locations that are likely affected by inter-regional or trans-boundary pollution events. More recently, however, new technologies and modelling capabilities have given rise to complimentary sources of information on air quality adding value to its monitoring. These include increased spatial coverage, with satellite remote sensing observations, city-wide analysis of pollutants at different heights in the atmosphere, with ground-based instrumentation, as well as attribution of increased pollutant levels to the original emitting sources, with state-of-the-art regional chemical transport modelling.

In this work, the tropospheric NO_2 concentrations will studied as air quality indicator. On a global scale, emissions of nitrogen oxides (NO_x=NO + NO_2) from natural sources far outweigh those generated by human activities (e.g. Seinfeld and Pandis, 2016). Natural sources include microbial processes in soils, oxidation of biogenic ammonia, wild fires and lightning. However, the NO_2 levels attributable to natural NOx emissions sources, typically referred to as background, are rather small compared to the magnitude of anthropogenic emissions. Currently, fossil fuel combustion is the largest source of NOx and, together with biomass burning emissions, anthropogenic activities dominate the NOx budget. As a trace gas with a relatively short lifetime, NO_2 is usually confined to a local scale with respect to its source and therefore exhibits strong spatial and temporal variations, rendering its monitoring dependent on the spatiotemporal resolution of its observations.

In the following, we aim to demonstrate the abilities, benefits, as well as limitations, of three different air quality-related pools of information, namely the Sentinel-5Precursor TROPOspheric Monitoring Instrument (TROPOMI) space-born observations, the Multi-Axis Differential Optical Absorption Spectroscopy (MAX-DOAS) ground-based measurements and the LOng Term Ozone Simulation – EURopean Operational Smog (LOTOS-EUROS) chemical transport modelling system. Using as case studies the Greek cities of Thessaloniki, population 1 million, and Ioannina, population 110 thousand, and the tropospheric NO_2 concentrations as air quality indicator, the local air quality levels and patterns between 2018 and 2021 are studied. These two cities are selected as two study cases representative of a large and a medium-sized urban agglomeration, exhibiting different characteristics regarding the strength and the nature/type of emission sources, as well as their individual geomorphology and topography. The aim in this work differs in that typically seen in literature, that of directly inter-comparing, validating, merging and contrasting the observations and simulations, as we aim to treat each dataset as autonomous and, without disregarding their differences, clearly present the common air quality picture that they provide.

In Section 2, both observational datasets and the model simulations are briefly described alongside the pre-processing of the original datasets specific to the requirements of this study. In Section 3, the findings per city are separately expanded and analysed. In Section 4, an executive summary of this work is provided alongside suggestions for future semi-operational use of these monitoring systems, with ideas that stemmed during this research.

2. Materials and Methods

Two Northern Greece cities

Thessaloniki, **Figure 1** (a), a port city located at the North of Greece, is the second largest city of the country, with over one million inhabitants in its metropolitan area, while

Preprints (www.preprints.org) | NOT PEER-REVIEWED | Posted: 27 April 2022 doi:10.20944/preprints202204.0257.v1

the majority of industrial activity is concentrated at the west and north-west part of the city. The meteorological features affecting air quality in the city are defined by the gulf of Thermaikos and the mountain on Hortiatis, causing both sea and land breeze and valley mountain winds (Moussiopoulos et al, 2006.) Road transport and industrial emissions are the two main sources of NOx emissions at the greater area of Thessaloniki (Poupkou et al., 2011) while according to Fameli and Asimakopoulos (2015) these two anthropogenic emission sources of Thessaloniki contribute by 35 ± 8 % and 45 ± 3 %, respectively, to the annual mean NOx emissions for Greece. Moussiopoulos et al., 2009, reported than even small reductions in NOx emissions (~5%) are sufficient for the NO_2 annual average to remain below the EU limit of 40 μg/m^3. The recent lockdown due to the Severe Acute Respiratory Syndrome Coronavirus-2, COVID-19, has offered the unique possibility to quantify NOx emissions changes due to transport. Koukouli et al., 2021, based on satellite observations and chemical transport modelling simulations, reported an ~10% reduction in NO_2 levels over the city while Akritidis et al., 2021, using a machine learning technique and measurements from two traffic air quality monitoring stations, reported a mean reduction of ~22%. These findings appear counter-intuitive since, in terms of the number of vehicles circulating in Thessaloniki, private cars and motorcycles are the vast majority. However, Liora et al., 2022, have recently shown that a significant decrease in the concentrations of atmospheric pollutants related to road traffic, reaching up to − 65% for NOx levels, is achieved when public buses circulating in a major road axis of Thessaloniki are replaced with battery electric vehicles. They conclude that both a reduction of the circulation of private vehicles by − 20% in combination with the use of battery electric vehicles for public transportation is the best scenario for an improved air quality in the city.

Ioannina, **Figure 1** (b), a town of ~110,000 habitants, is located in a plateau of about 480 m height, surrounded by four mountains and a lake. With respect to NO_2 levels, the air quality of the city is characterized by a "good" air quality index, as per the Index of Air Pollution from the European Commission (Sindosi et al., 2019) while a small weekend effect is also reported, with Sundays appearing as the cleanest days. A rather weak seasonal variability was also found for Ioannina; during summertime, two counteracting factors affect the local NO_2 levels, the absence of rain preventing NO_2 deposition, whereas the available solar radiation favours its destruction to O_3 formation. The city is however known, in recent years, to suffer from residential wood burning emissions, leading to persistent wintertime smog episodes (Stavroulas et al., 2020).

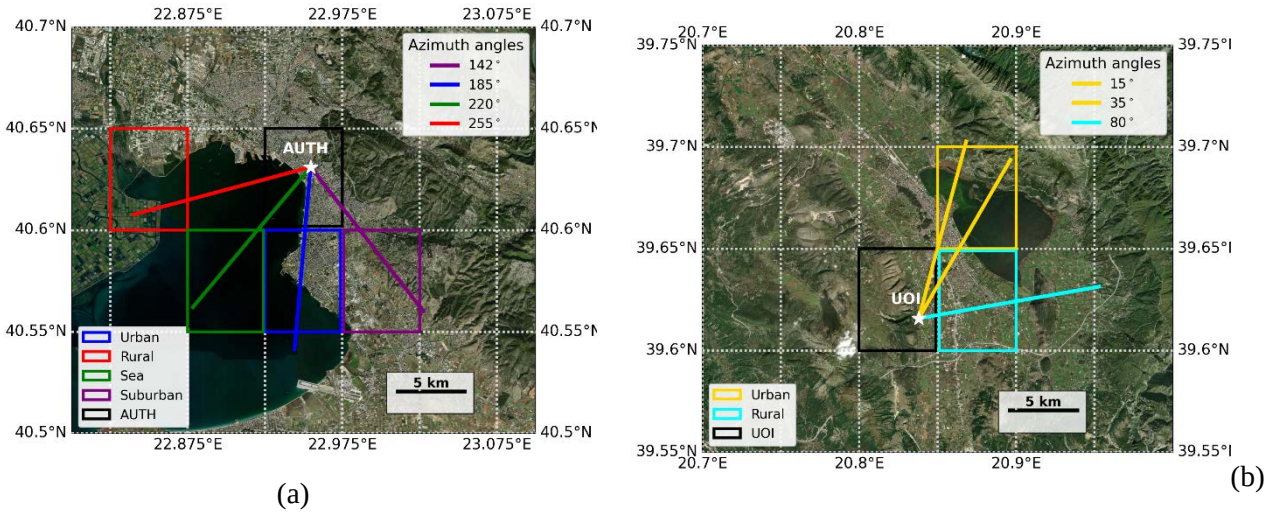

Figure 1. The Thessaloniki (a) and Ioannina (b) urban areas, including the location of the MAX-DOAS instrument and their respective viewing geometries.

 doi:10.20944/preprints202204.0257.v1

MAX-DOAS measurements

Multi-axis differential optical absorption spectroscopy (MAX-DOAS) is a ground-based passive remote sensing technique that is widely used for the detection of aerosols and trace gases in the Planetary Boundary Layer (PBL) and in the lowermost free troposphere (e.g., Pinardi et al., 2013; Wang et al., 2017; Chan et al., 2020). MAX-DOAS systems perform spectrally resolved measurements of scattered sunlight in the ultraviolet (UV) and visible (VIS) parts of the electromagnetic spectrum at different elevation angles (Hönninger et al., 2004). The spectral analysis of the recorded spectra by differential optical absorption spectroscopy (DOAS) (Platt and Stutz, 2008) allows the simultaneous detection of several trace gases that have distinct absorption structures, such as NO_2, formaldehyde (HCHO), O_3, sulfur dioxide (SO_2), water vapor (H_2O) and glyoxal (CHOCHO). The primary retrieved product from a MAX-DOAS system is the differential Slant Column Density (dSCD), i.e., the difference in trace gas column amount between a measured spectrum and a Fraunhofer reference spectrum (FRS), typically measured at the zenith. By recording spectra at different elevation angles (typically from close to the horizon towards the zenith) that belong to the same azimuth viewing direction, MAX-DOAS systems allow the retrieval of the trace gases vertical distribution in the lower troposphere.

Several MAX-DOAS systems (Phaethon) have been operating since 2014 on the rooftop of the Physics Department building of the Aristotle University of Thessaloniki (40.634° N, 22.956° E). The instruments have been gradually upgraded ever since for the retrieval of tropospheric NO_2 Vertical Column Densities (VCDs) (Drosoglou et al., 2017, 2018), total ozone columns (Gkertsi et al., 2018) and recently for the retrieval of aerosol and trace gas vertical profiles (Karagkiozidis et al., 2022). In the current study, scattered radiation spectra are measured at eleven elevation angles (i.e., 1, 2, 3, 4, 5, 6, 8, 10, 12, 15 and 30°) with an integration time of ~1 min per angle and a sequential zenith-sky measurement is used as the FRS for the retrieval of the NO_2 dSCDs. The dSCDs are calculated with the QDOAS (version 3.2, September 2017) spectral fitting software suite (https://uv-vis.aeronomie.be/software/QDOAS/, last access: 11 April 2022) and the NO_2 vertical profiles are retrieved by applying the Mexican MAXDOAS Fit (MMF) (Friedrich et al., 2019) inversion algorithm to the measured NO_2 dSCDs. Details about the instrumentation, the slant column retrieval settings and the input parameters for the inversion algorithm can be found in Karagkiozidis et al., 2022. One year of measurements between May 2020 to May 2021 over Thessaloniki is considered in this work, with the system configured to measure at four azimuth viewing directions, i.e., 142, 185, 220, and 255°, illustrated in **Figure 1**a as the different coloured lines. Depending on the known local NO_2 sources, these viewing directions roughly translate into a suburban (142°), an urban (185°), a sea (220°) and a rural location (255°). As will be discussed in the results section, the variability of the MAX-DOAS observations in the different azimuth viewing directions was found to be high. As a result, no clear distinction between the expected NO_2 loads could be differentiated, and the MAX-DOAS observations for the different azimuth viewing directions were averaged into one mean NO_2 time series.

During the PANhellenic infrastructure for Atmospheric Composition and climatE chAnge (PANACEA; https://panacea-ri.gr/) measurement winter campaign 2020, a MAX-DOAS system was installed on the rooftop of the Physics Department building at the University of Ioannina from 03 January 2020 until 18 February 2020. No remote sensing instruments operate regularly in Ioannina and the air quality is monitored only by in situ measurement sites that are distributed around the city centre. Tropospheric NO_2 VCDs are retrieved for the first time in Ioannina using MAX-DOAS observations. The system was configured to perform elevation scans at three azimuth viewing directions (15, 35 and 80°, illustrated in **Figure 1**b). The azimuth directions of 15° and 35° point towards the urban direction, while the 80° azimuth direction points to a suburban area. The viewing directions at elevation angles close to the horizon (i.e. less than 4°) are blocked by the surrounding mountains at all azimuths and thus NO_2 vertical profiles cannot be reliably retrieved. Hence, the NO_2 VCDs for Ioannina are derived from the dSCDs measured at 30

and 15° elevation angles by division with appropriate differential Air Mass Factors (dAMFs) that were calculated based on Radiative Transfer Model (RTM) simulations, taking into account the viewing geometry, the aerosol optical properties, and the instrument's viewing direction relative to the sun (Drosoglou et al., 2017). The NO_2 dSCDs at these elevation angles are lower than those measured at lower elevation angles and the associate fitting errors are larger. Furthermore, the NO_2 levels measured in Ioannina are considerably lower than in Thessaloniki and the differential optical densities are usually very low, reaching the spectrometer's detection limit. Hence, in order to obtain data of higher quality, the NO_2 VCDs are calculated from the average VCDs at 30 and 15° when those agreed to at least within 50%. Similarly as for Thessaloniki, for Ioannina, one azimuth-averaged MAX-DOAS time series is analysed.

S5P/TROPOMI observations

The Sentinel 5 Precursor (S5P) mission is a low Earth orbit polar satellite system to provide information and services on air quality, climate and the ozone layer in the timeframe between 2016 and 2023. The S5P satellite was launched on October 13th, 2017, carrying the TROPOspheric Monitoring Instrument, TROPOMI (Veefkind, et al., 2012). TROPOMI is a double channel, nadir-viewing grating spectrometer, measuring solar backscattered earthshine radiances in the ultraviolet, visible, near-infrared, and shortwave infrared with global daily coverage (van Geffen et al., 2019; 2020). The instrument has a swath width of 2600 km with a near nadir resolution at 3.5 x 5.5 km^2 since 6th August 2019 (3.5 x 7 km^2 initial spatial resolution). The wavelength range for the NO_2 column retrieval is between 405 and 465 nm and detailed information on the algorithm and data can be found in the TROPOMI NO_2 Algorithm Theoretical Basis Document (van Geffen et al., 2019; 2020). The data are constantly being validated by the Mission Performance Center Validation Data Analysis Facility, VDAF (https://mpc-vdaf.tropomi.eu/, last access: 16/9/2021). According to the latest validation report, TROPOMI L2_NO_2 tropospheric column data show a negative median bias of -34% when compared to MAX-DOAS ground based observations, well within the mission requirement of 50% (Quarterly Validation Report of the Copernicus Sentinel-5 Precursor Operational Data Products #11: April 2018-June 2021). This bias is reduced by approximately 20% when the MAX-DOAS profile data are vertically smoothed using the S5P averaging kernels.

In this work, we use offline v1.2 and v1.3 S5P/TROPOMI NO_2 tropospheric vertical column densities for a long sensing period, from May 2018 to March 2021, over the Greek cities of Thessaloniki and Ioannina. The data are filtered with a quality assurance value (qa_value>0.75) to ensure cloud free satellite observations and are gridded onto a 0.01° x 0.01° grid so as to extract the observations of the specified pixels required for this research. The day-of-week, monthly and seasonal variations of NO_2 are studied over urban, suburban, rural and sea areas in Thessaloniki and over urban and rural areas in Ioannina. In order to demonstrate the space-based monitoring capabilities more clearly, for Thessaloniki, the urban and suburban pixels were averaged into one, the sea and rural pixels into another and the central pixel over AUTH, where the bulk of the NOx emissions reside, is studied separately. Similarly, for Ioannina, the urban and suburban pixels are averaged while the central pixel over the UOI is studied separately.

LOTOS-EUROS simulations

LOTOS-EUROS is the chemical transport model used to simulate atmospheric pollutants in this study (Manders et al., 2017). The model is designed to simulate trace gases and aerosols in three dimensions in the lower atmosphere. LOTOS-EUROS is one of the state-of-the-art models used in the Copernicus Atmosphere Monitoring Service (CAMS, http://www.copernicus-atmosphere.eu) providing atmospheric information to a broad range of users, while it has been widely used in different studies concerning different

 doi:10.20944/preprints202204.0257.v1

parts of the world (e.g. Lopez-Restrepo et al., 2021; Blechschmidt et al., 2020). The model behaviour has been studied and validated over Greece and, for the city of Thessaloniki, it exhibits a mild underestimation of ~-10% when comparing simulated tropospheric NO_2 columns with S5P/TROPOMI and MAX-DOAS observations in summer (Skoulidou et al., 2021a).

The gas chemical mechanisms in LOTOS-EUROS are based on the updated version of CBM IV (Gery et al., 1989), while the secondary inorganic aerosols are represented by the ISORROPIA II module (Fountoukis and Nenes, 2007). The simulations were driven by operational meteorological data from the European Centre for Medium-Range Weather Forecasts (ECMWF) with a horizontal resolution of 7 km × 7 km. Atmospheric variables were simulated in 12 vertical layers expanding from the surface to about 200 hPa. The anthropogenic emission inventory used is based on CAMS-REG (CAMS regional European emissions) v4.2 inventory for the year 2017 and the temporal profiles used are the default profiles provided by CAMS for Europe. The CAMS-REG inventory provides European total annual gridded emissions on a 0.10° × 0.05° grid. The model calculates biogenic NO_x emissions from soils online, depending on soil type and temperature (Novak and Pierce, 1993.)

In this study, a nested domain configuration was used. Three different model runs with varying horizontal resolutions were performed so as to obtain a smooth transition on the dynamics from the large European scales to the desired local scale of the cities of Thessaloniki and Ioannina. First, a coarse resolution run that covers the region of Europe expanding from 15°W to 45°E and 30°N to 60°N and a horizontal resolution of 0.25°×0.25° was performed. The initial and boundary conditions in this run were derived from the CAMS global near-real-time (NRT) product with a spatial resolution of 35 km × 35 km. Secondly, a medium resolution run was performed over Greece (20° E to 27° E and 34° N to 42° N) with a horizontal resolution of 0.10° longitude × 0.05° latitude, while the boundary conditions in this case were retrieved from the lower-resolution domain. Finally, we performed two higher-resolution runs with a spatial resolution of 0.01° × 0.01°, covering the regions of Thessaloniki (22.775°E to 23.075°E and 40.5°N to 40.75°N) and Ioannina (20.7° E to 20.9° E and 39.55° to 39.85° N) deriving concentration of pollutants on an hourly basis, between April 2018 and April 2021. Concentrations of gases and aerosols simulated in the medium resolution run were used as boundary conditions for the runs of Thessaloniki and Ioannina.

While the aim of this work is not to validate the model simulations against the ground- and space-born observations, in order to have a homogeneous discussion, the simulations were also aggregated in the same manner as the space-born observations. I.e. for Thessaloniki, the urban and suburban pixels are shown as one, the sea and rural pixels as a second another and the central pixel over AUTH as a third. Similarly, for Ioannina, the urban and suburban pixels are averaged while the central pixel over the UOI is studied separately.

Table 1. The important characteristics of each dataset discussed in this work.

Dataset	Temporal resolution	Spatial resolution	Strong points	Limitations
TROPOMI/S5P	Once per day	3.5x5.5km pixel	High spatial coverage	Temporal coverage
MAX-DOAS	Every 15m in daylight	Point location, ~15km horizontal viewing	High temporal coverage	Spatial coverage
LOTOS-EUROS CTM	Every 1h	Depending on input parameters	High spatiotemporal coverage	Input information

In **Table 1**, the main characteristics of each dataset used in this work as air quality information pool are given, including their strong points and limitations. In such format, it becomes clearer that these are all complimentary to one another and each is an asset to any study performs on the urban scale.

Preprints (www.preprints.org) | NOT PEER-REVIEWED | Posted: 27 April 2022 doi:10.20944/preprints202204.0257.v1

3. Results

Thessaloniki metropolitan area

Spatial variability within the city

The average lifetime of NOx in the boundary layer depends on many factors like meteorological conditions, photolysis strengths, the duration of night-time, temperature, OH and H_2O concentrations. Typically, 2-6h are considered a good estimate for summer-time with this value reaching one day during winter-time and the absence of sunlight. As a result, a clear seasonality is expected especially between winter and summer loads. In **Figure 2**, the winter-time (left) and summer-time (right) TROPOMI tropospheric NO_2 concentrations are shown for Thessaloniki, including: the locations of urbanized areas (City Center, Pylaia, Kalamaria, Stavroupoli), the Port, the Airport, the heavily used Ring Road, the industrial area (Sindos) and a possible source of agricultural NOx emissions in the rice fields of Chalastra. The satellite data were hyper-gridded using standard space-born atmospheric analysis tools onto a 0.01x0.01° grid, however for the discussion below, these were aggregated according to the colour-coded 5x5 grid boxes. The centre of the city which includes the location of the MAX-DOAS system is depicted in black; with red, the two urban and suburban MAX-DOAS viewing geometries are shown and with green the rural and sea MAX-DOAS viewing geometries are represented [see **Figure 1**, left]. These same pixels are also be used in the analysis of the LOTOS-EUROS simulations. The time period between May 2018 and March 2020 is presented in this work, while TROPOMI typically overpasses between 11:00 and 12:00 UTC over Greece. Since this aim of this work is to demonstrate the individual dataset capabilities in monitoring air quality, and no to inter-compare them, no homogenization between them was applied. This is typically performed by the application of the averaging kernel information between different datasets who are sensitive at different altitudes within the atmosphere. Hence, the NO_2 reported levels are expected to vary in magnitude.

Over the entire domain shown, the wintertime loads range between 2.40 and 5.20x10^{15} molecules/cm^2, with a mean of 3.70±0.65x10^{15} molecules/cm^2 while the summer-time loads range between 1.45 and 2.45x10^{15} molecules/cm^2, with a mean of 1.88±0.24 x10^{15} molecules/cm^2. Furthermore, one already observes a clear distinction on the NO_2 loads in accordance to the expected emission locations annotated on the maps, discussed in the monthly mean time series with the next figure.

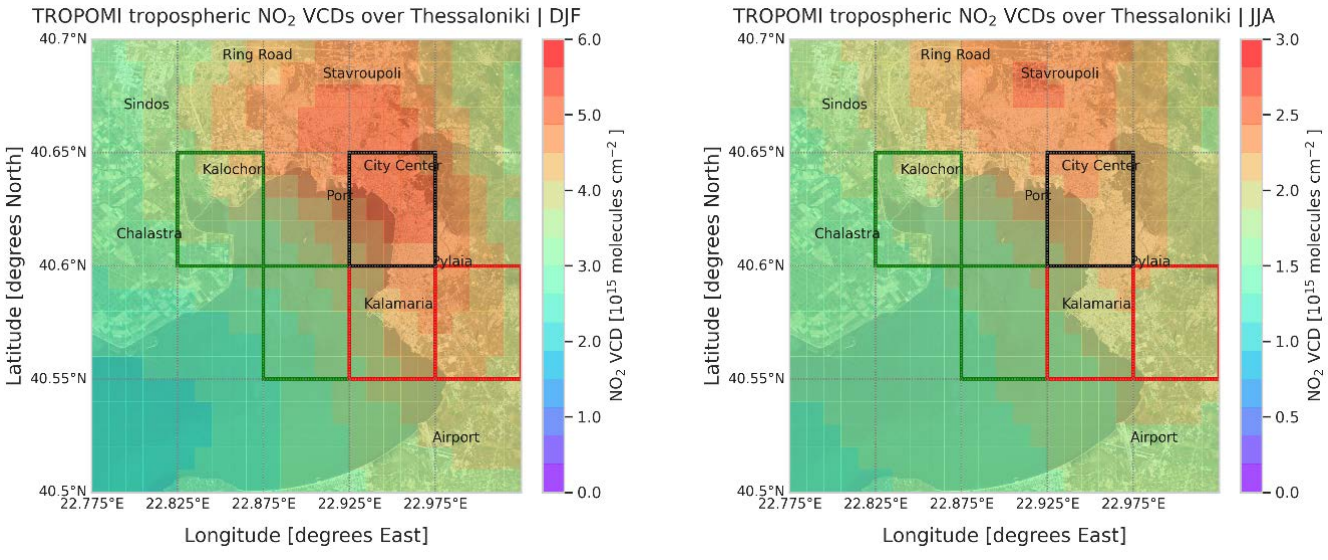

(a) (b)

Preprints (www.preprints.org) | NOT PEER-REVIEWED | Posted: 27 April 2022 doi:10.20944/preprints202204.0257.v1

Figure 2. TROPOMI tropospheric NO_2 seasonal load (10^{15} molecules/cm^2) over Thessaloniki during winter-time (a) and summer-time (b). Important locations of possible NO_2 emitting sources are also shown. Coloured cells represent the cells used in the analysis.

Time series and diurnal variability

The time series of the TROPOMI tropospheric NO_2 monthly mean loads (**Figure 3**) show a clear seasonal pattern for all locations studied, more pronounced for the city centre (black line) and the urban-suburban pixels (red line) than the rural-sea locations (green line) with the summer-time lows at the ~1.5x10^{15} molecules/cm^2 level and the winter-time highs at ~5.85, ~ 5.00 and ~4.15x10^{15} molecules/cm^2 level respectively. A curiously high load was observed for the month of February 2020, before COVID-19 related measures were enforced in Greece (Koukouli et al., 2020), which has been attributed to unusual meteorological conditions during that month, as also seen in the LOTOS-EUROS simulations, discussed in **Figure 5**a below.) Since the TROPOMI observations occur once per day, typically around 11:00-12:00 UTC over Thessaloniki, the shaded areas in the monthly mean time-series represent the spatial variability of the chosen pixels. This variability is small, hence further testifying to the ability of the satellite sensor in viewing the different NO_2 loads within the urban agglomeration.

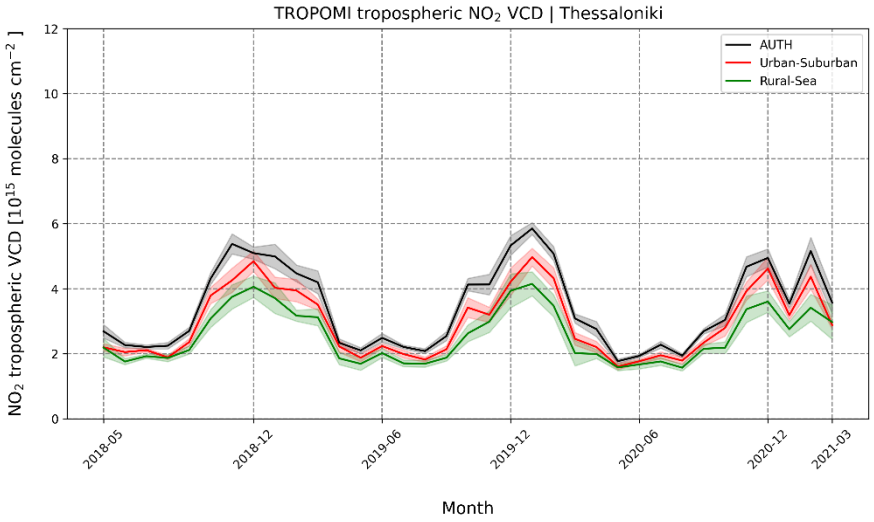

Figure 3. Monthly mean TROPOMI tropospheric NO_2 columns (10^{15} molecules/cm^2) over Thessaloniki for specific locations according to their known emission capabilities. The shaded areas represent the standard deviation of the spatial mean.

The MAX-DOAS monthly mean tropospheric NO_2 columns (10^{15} molecules/cm^2) over Thessaloniki (**Figure 4**a) are presented as an average of all the viewing geometries shown in **Figure 1**, left, for the same sensing time as that of TROPOMI. The variability of the MAX-DOAS observations between the different viewing geometries was rather large and does not permit an analysis per viewing geometry. The possible reason is the horizontal distance of the MAX-DOAS observations which span more than one 0.05x0.05° (~5x5km-pixels, ranging between 10-20km depending on season. This fact does not enable us to distinguish in statistical significance between the different locations around Thessaloniki from the MAX-DOAS observations. Hence, one averaged MAX-DOAS dataset is shown in this work. Overall, the MAX-DOAS reports lows around 5x10^{15} molecules/cm^2 for the summer-time and highs reaching ~12x10^{15} molecules/cm^2 in December, with a mean of 7.34±2.15x10^{15} molecules/cm^2, replicating the expected seasonal NO_2 pattern albeit with higher absolute values than the satellite sensor.

Preprints (www.preprints.org) | NOT PEER-REVIEWED | Posted: 27 April 2022 doi:10.20944/preprints202204.0257.v1

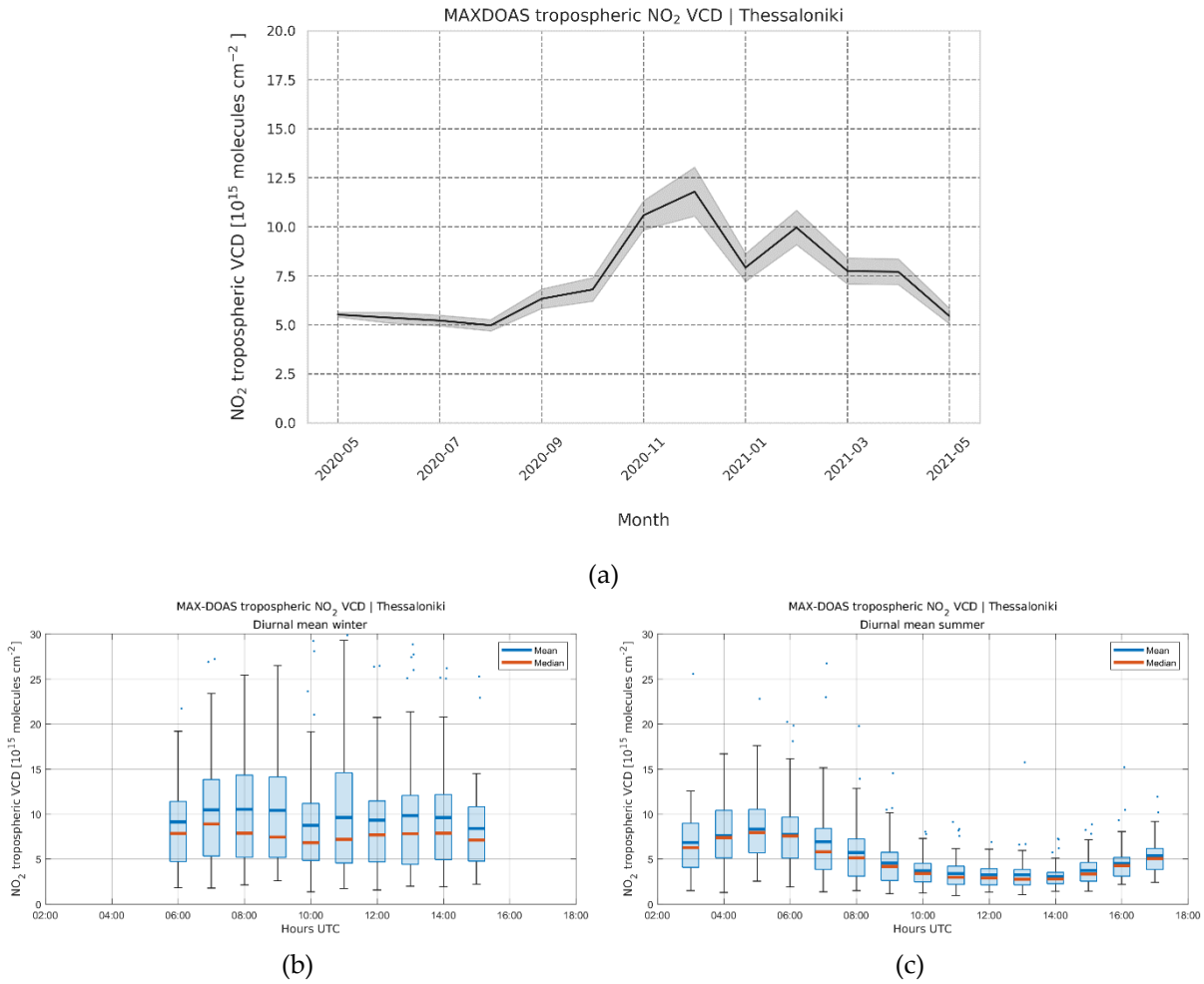

Figure 4. (a) Monthly mean MAX-DOAS tropospheric NO_2 columns (10^{15} molecules/cm^2) over Thessaloniki Thessaloniki. Diurnal variability during winter-time (b) and summer-time (c).

The ability of the MAX-DOAS system to measure through the daylight hours, one of the strengths of this observational system, permits the discussion of the diurnal pattern of the atmospheric gas. In **Figure 4b** the diurnal variability during winter time is presented, as a box-plot, while the summer-time is shown in **Figure 4c**. We note that during winter-time the mean levels remain high during the different sensing times, between ~6-7x10^{15} molecules/cm^2, with high variability as shown by the standard error bars and the marked difference between mean [in blue] and median [in red] levels. This picture is well expected as the photochemical destruction of NO_2 is weaker and the background levels of the species remain high, due to its increased life-time. During summer-time, the expected diurnal variability is very clear, with higher levels of ~7-8x10^{15} molecules/cm^2, during rush hour (~05:00-06:00 UTC) and lows (~3-4x10^{15} molecules/cm^2) after 10:00 UTC where sunlight is strong, with the secondary maximum appearing after 16:00 UTC where the photochemical NO_2 destruction has slowed down.

The LOTOS-EUROS CTM simulations over the different locations around Thessaloniki are in complete agreement with what the two observational sets have already revealed. In **Figure 5**a, the monthly mean time-series of the same pixels and same overpass time as shown for TROPOMI (**Figure 3**) also show lows during the summer time and highs

Preprints (www.preprints.org) | NOT PEER-REVIEWED | Posted: 27 April 2022 doi:10.20944/preprints202204.0257.v1

during the winter months, a clear distinction for the three different expected NO_2 concentrations, including the peak of February 2020. As the entire timeline of the CTM simulations depend on the same NO_2 emission inventory for year 2017, this February 2020 increase may only be attributed to the special meteorological conditions of that month and corroborate the findings of the TROPOMI observations.

In more detail, the city centre location hosting the MAX-DOAS instrument reports a seasonality between 4.0 and 10.5x10^{15} molecules/cm^2, with a mean load of 6.45±1.68x10^{15} molecules/cm^2, while the seasonality is similar for the urban-suburban and rural pixels, between 3.0 and 8.75x10^{15} molecules/cm^2, albeit with somewhat different mean loads: for the urban-suburban this was estimated to be 5.60±1.50x10^{15} molecules/cm^2 while for the rural location at 4.85±1.50x10^{15} molecules/cm^2. Recall that the standard deviations reported here, and shown as coloured shaded areas in the figures, represents the spatial variability of the hyper-grid and not a temporal variability.

Contrary to the satellite observations, which provide a picture of the situation for a specific time of day, and the MAX-DOAS observations, which provide the picture during daylight hours, the LOTOS-EUROS can provide estimates of the NO_2 concentrations throughout the entire day. Of course, the CTM simulations depend on accurate input parameters and the correct representation of different physicochemical processes within the model. The CTM diurnal variability for winter (**Figure 5**b) and summer (**Figure 5**c) revealed issues in the modelling system, already identified by Skoulidou et al, 2021.

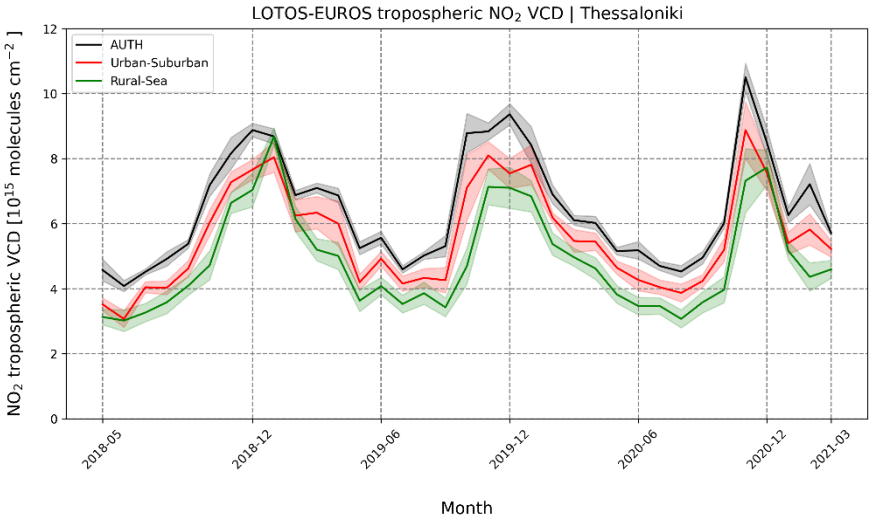

(a)

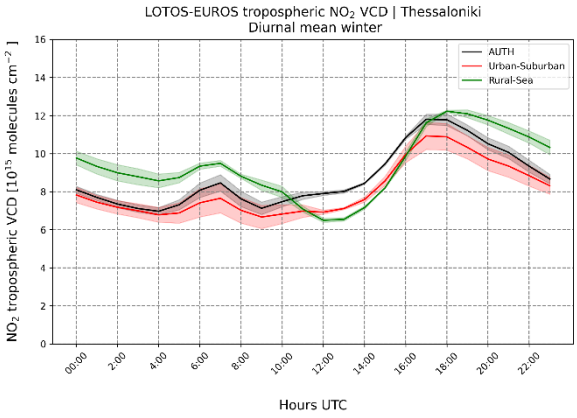

(b)

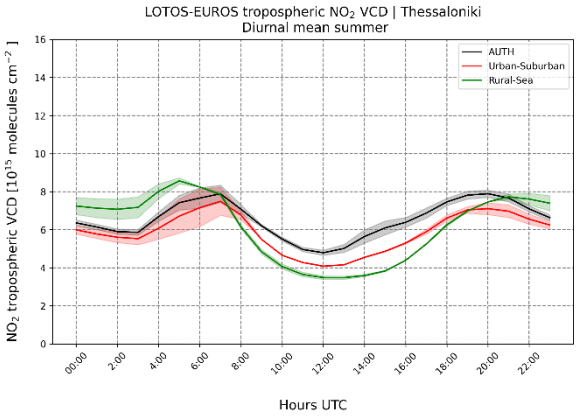

(c)

Figure 5. (a) Monthly mean LOTOS-EUROS tropospheric NO_2 columns (10^{15} molecules/cm^2) over Thessaloniki for specific locations as per **Figure 3**(a). Diurnal variability during winter-time (b) and summer-time (c).

The first point of interest, for the winter diurnal patterns, is the unexpected higher night-time NO_2 concentrations (after 16:00 UTC) which reach around 10-12x10^{15} molecules/cm^2 well over the daytime maximum of ~9x10^{15} molecules/cm^2. Skoulidou et al., 2021, validated LOTOS-EUROS surface NO_2 simulations against air quality monitoring stations around Athens and Thessaloniki. The night-time comparisons were the most difficult to interpret; during the night period, the model overestimates the low NO_2 measurements and underestimates the higher concentrations over the air quality stations. They concluded that the diurnal evolution of the boundary layer height appears to strongly affect both the mixing processes within the CTM and the photochemical NO_2 destruction strength. These two processes may well be responsible for the unexpectedly high night-time NO_2 concentrations for all locations examined during winter (**Figure 5**b). During summer (**Figure 5**c) a similar issue appears to occur, with the night-time max however only rising to the morning peak levels (~7-8x10^{15} molecules/cm^2), possibly due to the rapid NO_2 photochemical destruction.

The second point of interest is the model behaviour over the rural-sea pixel (green lines) both during winter-time (**Figure 5**b) and summer-time (**Figure 5**c). With the absence of known strong emission sources, the very high levels reported in winter starting during the night-time hours after 18:00 UTC and flowing into daytime hours up to 10:00 UTC, were entirely unexpected. In **Figure A1**, maps of the LOTOS-EUROS tropospheric NO_2 levels with colour-coded annotations of the locations of the pixels shown in **Figure 5**, are presented for winter and summer-time averaged for 00:00-06:00, 06:00-12:00, 12:00-18:00 and 18:00-24:00 UTC. It is clear that the rural and sea pixels both depict extremely high NO_2 levels during the entire day, apart during the peak of the strong photochemical processing during the daylight hours. This surprising finding is corroborated by the Copernicus Atmospheric Monitoring Service, CAMS, regional ensemble re-analysis publicly available via the European air quality | Copernicus Atmosphere Monitoring Service. While this feature will be further investigated in the future, we can already note that the large scale dominant wind patterns for the region, shown in **Figure A2**, do not appear to explain this behaviour in themselves. During winter-time, Northern winds are prominent throughout the day while during summer-time more variable wind patterns can be observed depending on the time of day. These wind fields depict the ECMWF meteorological fields provided in a 7x7km^2 resolution to the LOTOS-EUROS model. The topography of the bay of Thessaloniki is however known to host extremely complex wind patterns which greatly affect the photochemical processes, discussed extensively in Moussiopoulos et al., 2006. They reported moderate ozone levels for Thessaloniki throughout the day which are decisively affected by the break-up of the night-time temperature inversion and the onset of the sea breeze. Lessons learned from their work, which focusses on tropospheric O_3, will be used to investigate this phenomenon further.

Day-of-week variability

The day-of-week, or weekly, variability of tropospheric NO_2 has been examined in the past for major megacities on a global scale using different observational platforms. Beirle et al., 2003, studied the space-born Global Ozone Monitoring Experiment (GOME)/ERS-2 tropospheric NO_2 columns for industrialized regions and cities in the US, Europe and Japan and reported a clear Sunday minimum, of about 25–50% lower than working day levels. Stavrakou et al., 2020, using the more recent Ozone Monitoring Instrument (OMI)/Aura and S5P/TROPOMI observations also reported a minimum ranging between 25% and 38% for large cities globally, for the traditional resting day of Sunday. Focusing on the continental US, Golberg et al., 2021, using only the high spatially resolution S5P/TROPOMI observations found that Saturday and Sunday NO_2 concentrations are

Preprints (www.preprints.org) | NOT PEER-REVIEWED | Posted: 27 April 2022 doi:10.20944/preprints202204.0257.v1

16% and 24% lower, respectively, than during weekdays. These space-based dataset reports are well in line with the work of Wang et al., 2022, who used in situ air quality monitoring stations for the agglomeration of Los Angeles, USA, where a 30%–35% Sunday decline in NO_2 atmospheric content was reported.

Most of these studies focus on areas with a high anthropogenic NO_2 atmospheric load which is not the case for the two Greek cities discussed here. Ialongo et al., 2020, estimated that the S5P/TROPOMI tropospheric columns are about 20–30 % lower during weekends over Helsinki, Finland, while a ground-based spectrophotometer, Pandora, also showed lower values but only by about 10–20 %. In **Figure 6**, the wintertime (left column) and summer time (right column) day-of-week tropospheric NO_2 concentrations are shown for the TROPOMI observations (top row), the LOTOS-EUROS simulations (middle row) and the MAX-DOAS measurements (bottom row). Even though the relative magnitudes for the NO_2 concentrations differ greatly between the two seasons and type of dataset, the weekend effect is present in all three: TROPOMI reports a -20.2 ± 1.1% (-22.1 ± 2.5%) decline for Sunday, LOTOS-EUROS reports a -15.2 ± 2.1% (-7.8 ± 0.9%) and MAX-DOAS reports a -25.3% (-33.1%) during wintertime (summertime)

One further notes from **Table 2**, that larger NO_2 loads were sensed for Fridays with the LOTOS-EUROS CTM reporting the highest deviations of the weekly mean, at 10.5 ± 2.8% for winter and 6.0 ± 4.0% for the summer. The CTM results are attributed to the temporal profile used in the LOTOS-EUROS (Kuenen et al., 2014) which have recently been thoroughly updated (Kuenen et al., 2022) and discussed by Guevara et al, 2021. The resulting emissions are shown in **Figure A3**, where one notes the gradual increase of the input emissions between Monday and Friday, with a sharp drop for Saturday and even sharper for Sundays. An extensive analysis based on traffic count measurements at numerous locations around the Globe, including Athens, was developed for the road transport sector so as to calculate the monthly, weekly and hourly profiles required by the CTM. This increase is also reproduced by the TROPOMI observations which also show increased Friday loads by 15.7 ± 3.8% for winter and 10.0 ± 4.7% for summer.

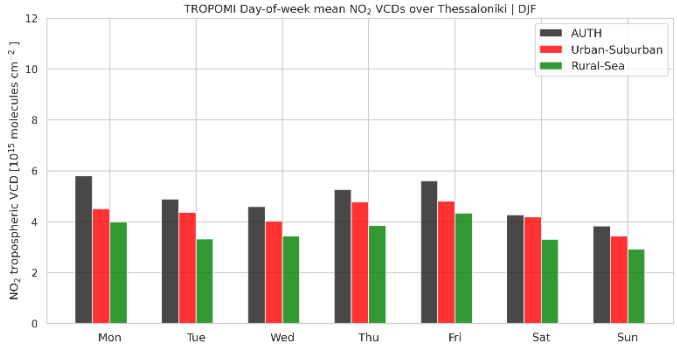

(a)

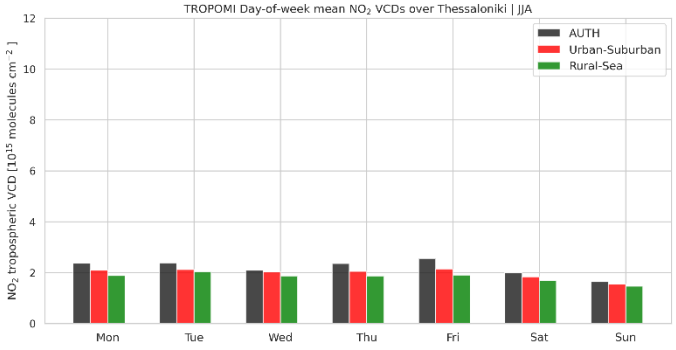

(b)

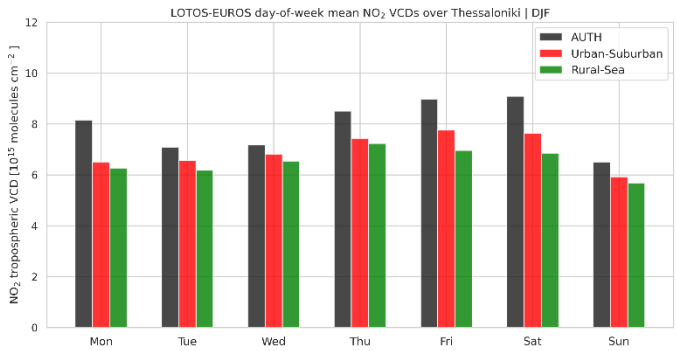

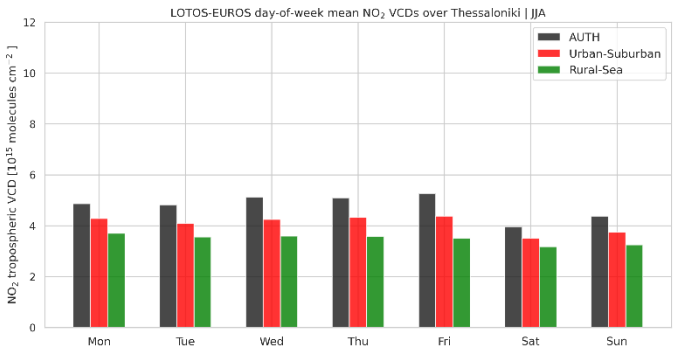

Preprints (www.preprints.org) | NOT PEER-REVIEWED | Posted: 27 April 2022 doi:10.20944/preprints202204.0257.v1

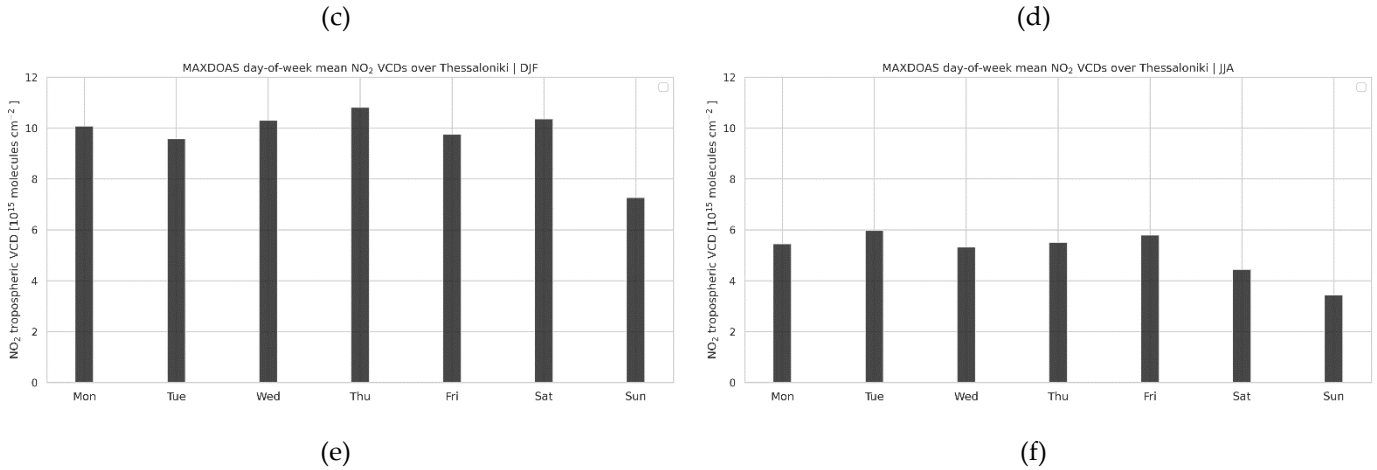

Figure 6. Day-of-week variability of tropospheric NO_2 columns (10^{15} molecules/cm^2) over Thessaloniki revealed by TROPOMI observations during wintertime (a) and summer time (b), LOTOS-EUROS simulations during wintertime (c) and summertime (d) and MAX-DOAS observations during wintertime (e) and summertime (f).

Table 2. The percentage deviation of day-of-week NO_2 columns from the weekly average for Thessaloniki. The std values represent the variability of the different locations sensed, where applicable.

		Monday	Tuesday	Wednesday	Thursday	Friday	Saturday	Sunday
Winter	TROPOMI	11.5 ± 5.5%	-2.1 ± 4.0%	-5.7 ± 1.0%	8.6 ± 1.8%	15.7 ± 3.8%	-7.8 ± 4.1%	-20.2 ± 1.1%
	LOTOS-EUROS	-2.5 ± 3.9%	-7.2 ± 2.4%	-3.8 ± 4.1%	8.3 ± 1.7%	10.5 ± 2.8%	9.8 ± 4.0%	-15.2 ± 2.1%
	MAX-DOAS	3.5%	-1.6%	5.8%	11.1%	0.2%	6.4%	-25.3%
Summer	TROPOMI	5.8 ± 1.7%	9.1 ± 1.9%	0.4 ± 3.6%	4.6 ± 2.0%	10.0 ± 4.7%	-7.7 ± 1.2%	-22.1 ± 2.5%
	LOTOS-EUROS	4.3 ± 2.0%	1.1 ± 0.9%	4.8 ± 1.7%	5.0 ± 1.6%	6.0 ± 4.0%	-13.4 ± 3.7%	-7.8 ± 0.9%
	MAX-DOAS	6.2%	16.4%	3.6%	7.2%	13%	-13.4%	-33.1%

Ioannina city and environs

Spatial variability within the city

Ioannina, a medium sized-city with no industrial zone, is exhibiting as expected far lower tropospheric NO_2 loads than Thessaloniki. In **Figure 7**, the TROPOMI-reported NO_2 levels are presented for the wintertime (left) and the summer time (right) including the location of the University of Ioannina, UOI, where the MAX-DOAS instrument was placed during the PANACEA winter campaign, the City Centre, the small provincial airport as well a sub-urban location (Anatoli) and a rural location (Kastritsa.) Over the entire domain shown, the wintertime loads range between 1.02 and 2.02x10^{15} molecules/cm^2, with a mean of 1.33±0.23x10^{15} molecules/cm^2 while the summertime loads range between 0.90 and 1.20x10^{15} molecules/cm^2, with a mean of 1.04±0.06 x10^{15} molecules/cm^2. The locations of the pixels chosen for further discussion are shown in red, for the urban-suburban locations and two of the MAX-DOAS viewing angles and in green, for the rural location and the third MAX-DOAS viewing angle.

Preprints (www.preprints.org) | NOT PEER-REVIEWED | Posted: 27 April 2022 doi:10.20944/preprints202204.0257.v1

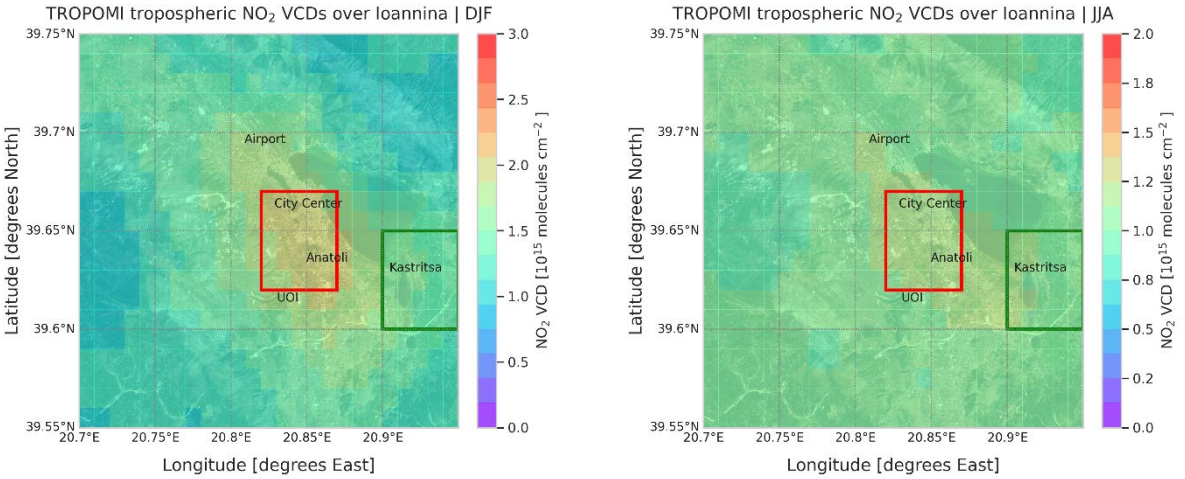

(a) (b)

Figure 7. TROPOMI tropospheric NO_2 seasonal load over Ioannina in winter-time (a) and summer-time (b). Important locations of possible NO_2 emitting sources are also shown. Coloured cells represent the cells used in the analysis.

Time series and diurnal variability

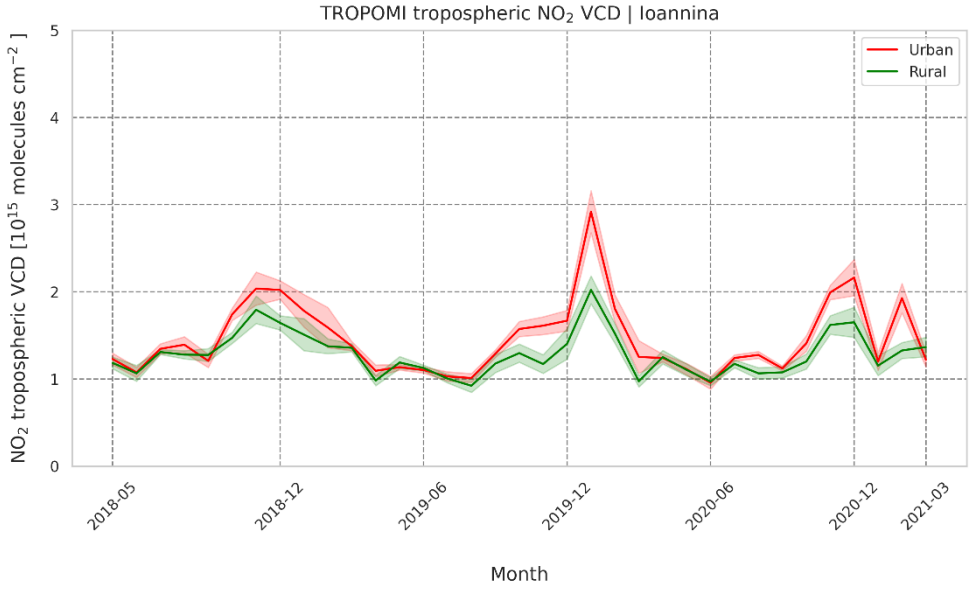

Figure 8. Monthly mean TROPOMI tropospheric NO_2 columns (10^{15} molecules/cm^2) over Ioannina for specific locations according to their known emission capabilities. The shaded areas represent the standard deviation of the spatial mean.

When focusing on the two urban and rural pixels, a distinction between the tropospheric NO_2 columns becomes clearer, especially for the wintertime months. For the urban pixels, which encompass the city of Ioannina and the main sub-urban location, the monthly mean time series of the TROPOMI observations (**Figure 8**, red line) show summertime lows at ~1.0x10^{15} molecules/cm^2 and wintertime highs at ~3.0x10^{15} molecules/cm^2 with mean annual loads of 1.44±0.43x10^{15} molecules/cm^2. For the rural pixel, in green, the

Preprints (www.preprints.org) | NOT PEER-REVIEWED | Posted: 27 April 2022 doi:10.20944/preprints202204.0257.v1

summertime lows are ~ 0.67x10^{15} molecules/cm^2, the wintertime highs at ~2.02x10^{15} molecules/cm^2 and the mean annual load at 1.27±0.26x10^{15} molecules/cm^2. The February 2020 relatively high NO_2 load, already identified for Thessaloniki, appears over Ioannina as well.

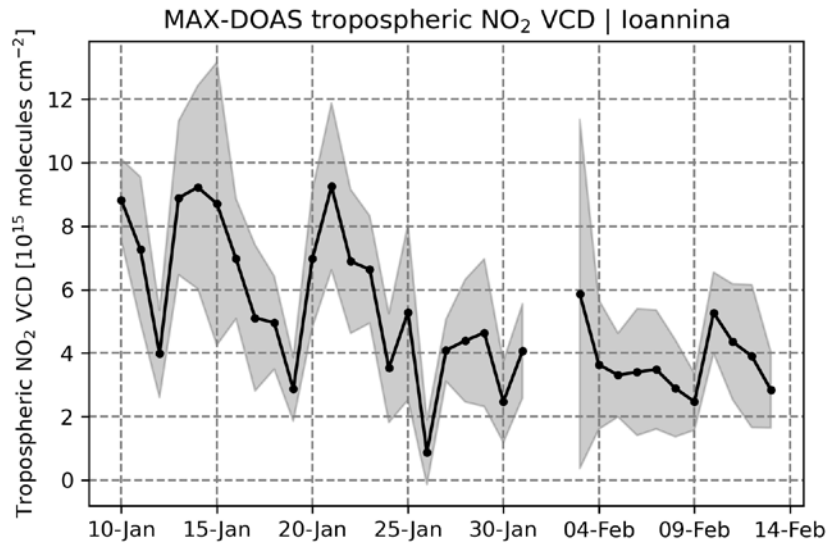

(a)

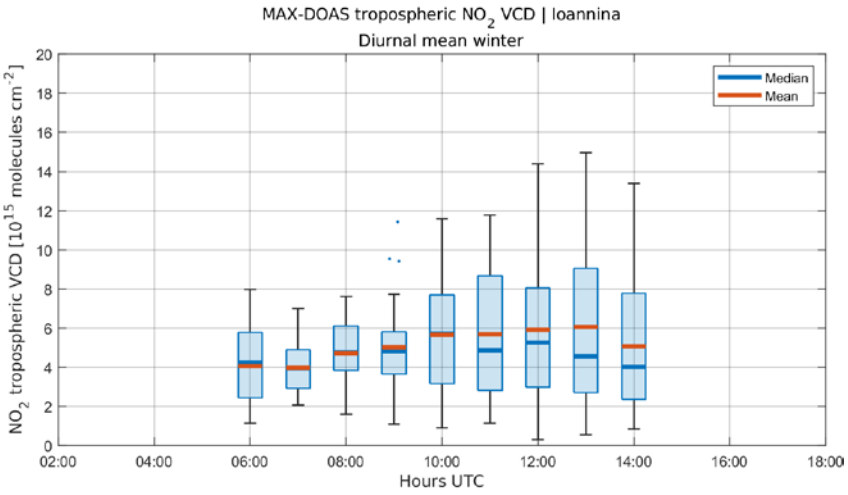

(b)

Figure 9. (a) Daily mean time series of MAX-DOAS tropospheric NO_2 columns (10^{15} molecules/cm^2) during winter-time over Ioannina. (b) The respective diurnal variability.

Due to the short time that the PANACEA campaign took place in Ioannina, the MAX-DOAS observations are limited to January and February 2020. From **Figure 9**a, where the daily mean observed tropospheric NO_2 columns are shown, one notes that in the beginning of the PANACEA campaign the overall load over Ioannina was on average ~6.6x10^{15} molecules/cm^2 while the second part, after January 25th, the average load was ~3.65x10^{15} molecules/cm^2. The shaded areas represent the variability of the hourly observations. In **Figure 9**b, the winter-time diurnal NO_2 levels sensed by the MAX-DOAS are presented between 06:00 and 14:00 UTC, the full daytime hours. The increase in NO_2 levels, between ~4 to ~6x10^{15} molecules/cm^2), in the morning hours does not seem to abate, but rather levels remain high throughout the afternoon hours as well. The afternoon levels have a high

Preprints (www.preprints.org) | NOT PEER-REVIEWED | Posted: 27 April 2022 doi:10.20944/preprints202204.0257.v1

variability associated with them, showing a very similar picture as what is measured by an in situ air quality monitoring station operating on location (not shown here).

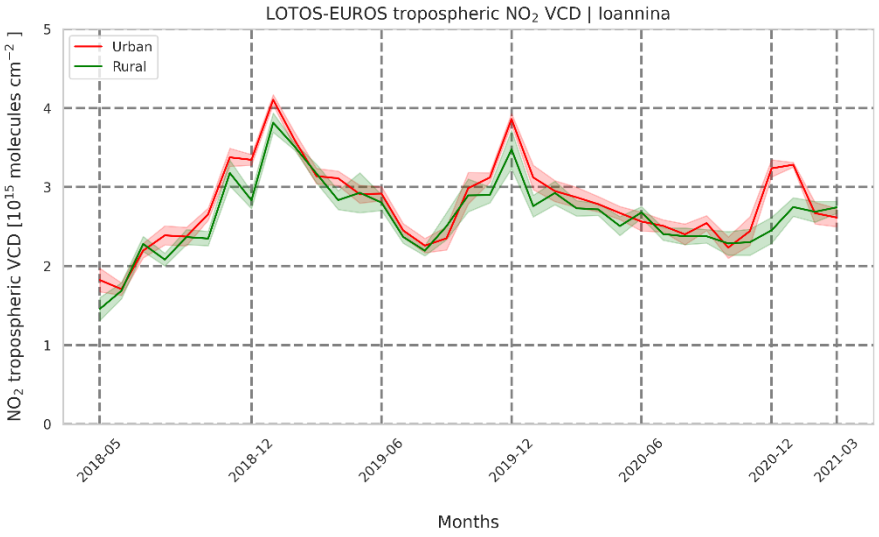

(a)

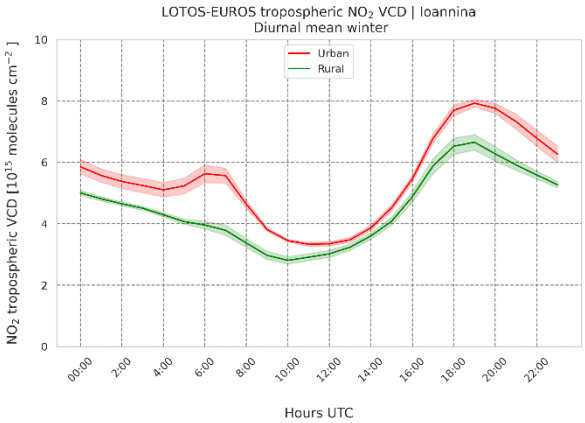

(b)

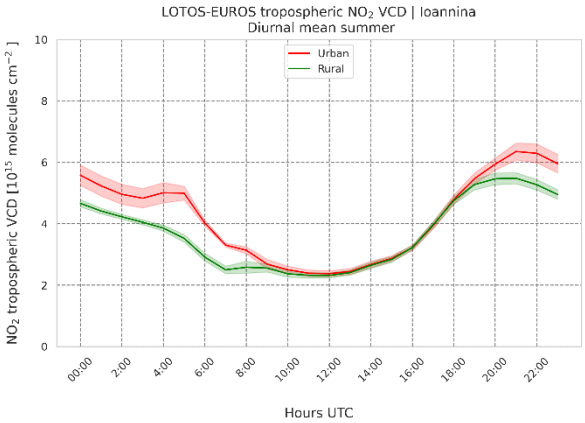

(c)

Figure 10. (a) Monthly mean LOTOS-EUROS tropospheric NO_2 columns (10^{15} molecules/cm^2) over Ioannina for specific locations as per **Figure 3**(b). Diurnal variability during winter-time (b) and summer-time (c).

A similar seasonal variability with higher overall NO_2 levels as observed by TROPOMI is simulated by the CTM (**Figure 10**a) with summertime lows around 2x10^{15} molecules/cm^2, and winter-time highs between 3-4x10^{15} molecules/cm^2, depending on the year. The difference between the urban and rural locations is not so high, and in most cases within the spatial variability of the simulations. The LOTOS-EUROS diurnal variability in the case of Ioannina, shown for winter in **Figure 10**b and for summer in **Figure 10**c, presents an expected evolution with a double-peak in the urban locations in the morning and evening. The wintertime evening levels are, as for the case of Thessaloniki, higher than the morning traffic-related levels and merit further investigation as to the exact physico-chemical processes that are driving these night-time increases.

Day-of-week variability

Preprints (www.preprints.org) | NOT PEER-REVIEWED | Posted: 27 April 2022 doi:10.20944/preprints202204.0257.v1

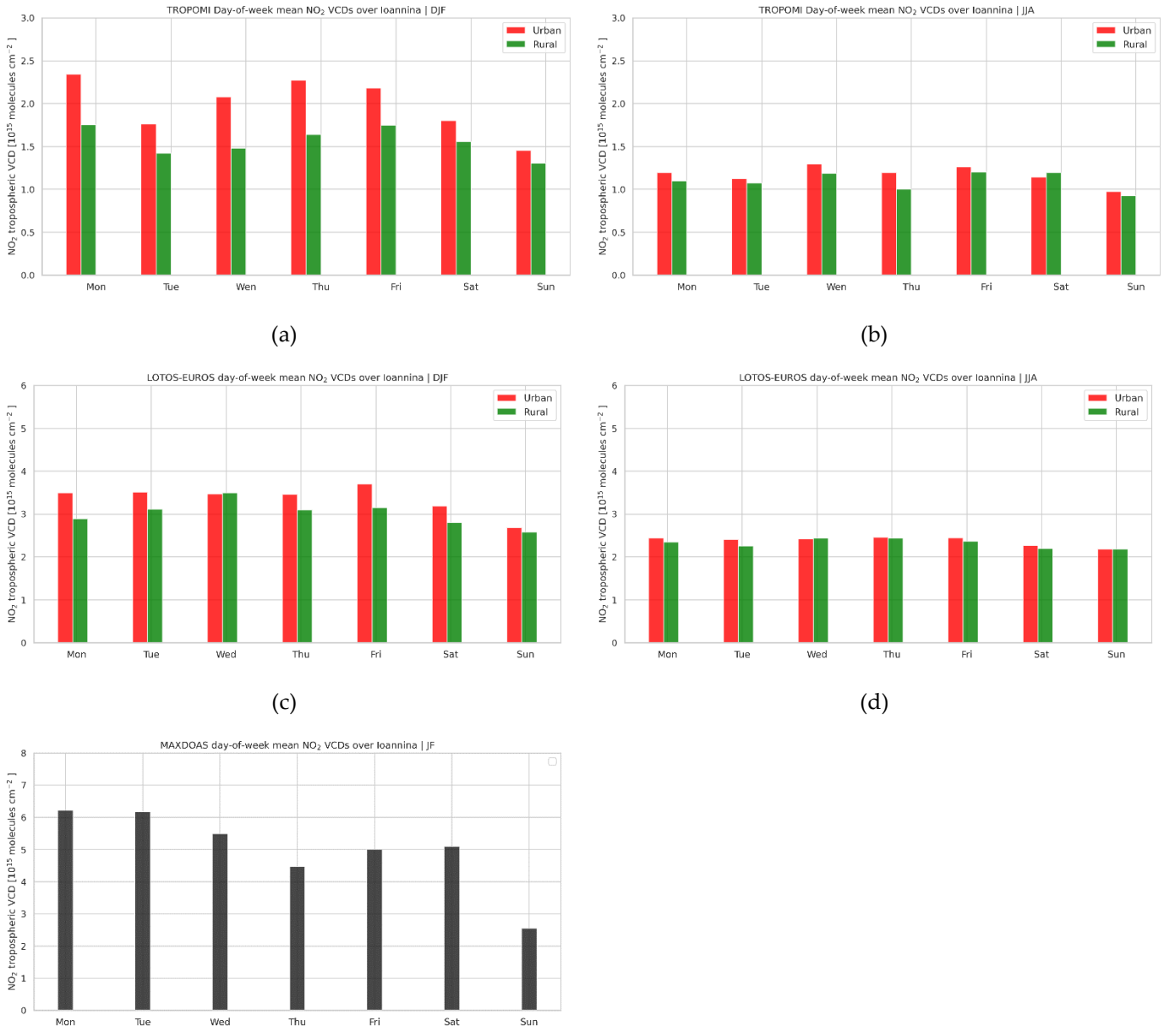

Figure 11. Day-of-week variability of tropospheric NO_2 columns (10^{15} molecules/cm^2) over Ioannina revealed by TROPOMI observations during wintertime (a) and summer time (b), LOTOS-EUROS simulations during wintertime (c) and summertime (d) and MAX-DOAS observations during wintertime (e).

The day-of-week variability over Ioannina (**Figure 11**) follows the same patterns as for Thessaloniki, with the lowest tropospheric NO_2 columnar value deviations reported for Sunday by all three data sources, with a different magnitude. The wintertime (left column) and summer time (right column) day-of-week tropospheric NO_2 concentrations are shown for the TROPOMI observations (top row), the LOTOS-EUROS simulations (middle row) and the MAX-DOAS measurements (bottom row). The weekend effect is present in all three: TROPOMI reports a -16.3 ± 0.5% in winter (-21.5 ± 5.2% in summer) decline for Sunday, LOTOS-EUROS reports corresponding declines of -17.3 ± 2.8% in winter (-6.8 ± 1.2% in summer) and MAX-DOAS reports a very strong Sunday decrease, at -49%, which is based on five Sundays during winter 2020. All statistics are reported in **Table 3**.

Preprints (www.preprints.org) | NOT PEER-REVIEWED | Posted: 27 April 2022 doi:10.20944/preprints202204.0257.v1

Table 3. The percentage deviation of day-of-week NO_2 columns from the weekly average for Ioannina. The std values represent the variability of the different locations sensed, where applicable.

		Monday	Tuesday	Wednesday	Thursday	Friday	Saturday	Sunday
Winter	TROPOMI	1.1 ± 1.1%	-2.9 ± 1.0%	9.4 ± 1.2%	-3.3 ± 5.5%	8.6 ± 0.7%	3.4 ± 5.6%	-16.3 ± 0.5%
	LOTOS-EUROS	-0.1 ± 4.2%	3.9 ± 0.8%	9.5 ± 6.3%	2.8 ± 0.2%	7.3 ± 2.8%	-6.2 ± 1.1%	-17.3 ± 2.8%
	MAX-DOAS	24.4%	23.4%	9.8%	-10.7%	0.1%	2%	-49%
Summer	TROPOMI	15.2 ± 2.8%	-10.0 ± 1.3%	-0.1 ± 4.8%	9.8 ± 4.7%	11.1 ± 1.2%	-4.6 ± 4.6%	-21.5 ± 5.2%
	LOTOS-EUROS	2.0 ± 0.9%	-0.6 ± 1.9%	3.6 ± 1.6%	4.4 ± 0.8%	2.4 ± 0.5%	-5.0 ± 0.3%	-6.8 ± 1.2%
	MAX-DOAS	n/a						

4. Conclusions

In this work, the air quality due to nitrogen dioxide levels over two Northern Greek cities has been studied using Sentinel-5Precursor TROPOspheric Monitoring Instrument (TROPOMI) space-born observations, Multi-Axis Differential Optical Absorption Spectroscopy (MAX-DOAS) ground-based measurements and the LOng Term Ozone Simulation – EURopean Operational Smog (LOTOS-EUROS) chemical transport modelling system simulations. Each of these systems offers a different perspective to the current air quality situation over Thessaloniki and Ioannina depending on their spatiotemporal monitoring capabilities of the tropospheric NO_2 levels. While these levels differ in magnitude between the two cities, following the different magnitudes of their NOx emitting sources, a common picture emerges as follows:

- A clear seasonal pattern, with high NO_2 levels during winter-time and lower NO_2 levels in summer was found, clearly reflecting the effect of the high photochemistry strengths during the mainly sunlight summer months over Greece, by all three systems.
- A marked distinction between locations with high emitting sources and clean locations around the urban sprawl were reported by both the space-born observations and the model simulations.
- The expected NO_2 diurnal variability, less pronounced during winter-time but quite strong during summer-time, was seen in both the ground-based measurements as well as the model simulations.
- All three systems identified a discernible day-of-week variability with the lowest levels reported for Sundays in both seasons, reflecting the effect of reduced traffic emissions in both Greek cities.

Furthermore, the following open questions were identified and are thought to merit further investigation in the future:

- The effect of the small scale wind patterns around the city of Thessaloniki and its bay was divulged in both the space-born observations and the model simulations. The continuous transport of the pollutant in nearby locations may be responsible for a constant background NO_2 level, which cannot be assessed by the air quality monitoring stations that are located within the city boundaries.
- Extremely high NO_2 levels during the night-time hours are simulated by the CTM which were unexpected considering the relatively low NO_2 loads over the two cities were reported for the first time. The main physicochemical mechanism behind these enhancements should be investigated so as to assess its representativeness to the true situation.

The launch of the EUMETSAT Sentinel-4 UVN (Ultra-violet Visible Near-infrared) imaging spectrometer on the geostationary MTG-S platform in early 2024 will offer a complete hourly space-born observational dataset that will undoubtedly provide further insights on the air quality status over Greece.

Preprints (www.preprints.org) | NOT PEER-REVIEWED | Posted: 27 April 2022 doi:10.20944/preprints202204.0257.v1

Author Contributions: Conceptualization, D. B. and A. B.; methodology, M.E.K. and D.B.; software, A.P and M.E.K.; validation, D.K. and I.S.; investigation, A.P. and I.S.; data curation, M.E.K, A. P. and D.K.; writing—original draft preparation, M.E.K.; writing—review and editing, A.P and I.S.; supervision, D.B. All authors have read and agreed to the published version of the manuscript.

Funding: This research has been financed by the European Union (European Regional Development Fund) and Greek national funds through the Operational Program "Competitiveness, Entrepreneurship and Innovation" (NSRF 2014-2020) by the "Panhellenic Infrastructure for Atmospheric Composition and Climate Change" project (MIS 5021516) implemented under the Action "Reinforcement of the Research and Innovation" Infrastructure.

Institutional Review Board Statement: Not applicable.

Informed Consent Statement: Not applicable.

Data Availability Statement: The S5P/TROPOMI observations are publicly available from the Copernicus Open Access Hub (https://scihub.copernicus.eu/, ESA, 2022). The LOTOS-EUROS CTM simulations shown in this work are performed with the open source version v02.02.001 and are available upon request from A.P. The MAX-DOAS observations are available upon request from D.K.

Acknowledgments: We would like to wholeheartedly thank Dr. Astrid Manders and Dr. Arjo Segers, TNO, Climate, Air and Sustainability, Utrecht, the Netherlands, for their valuable advice on the LOTOS-EUROS CTM. Results presented in this work have been produced using the Aristotle University of Thessaloniki (AUTH) High Performance Computing Infrastructure and Resources. The authors would like to acknowledge the support provided by the AUTH IT Centre throughout the progress of this research work. We further acknowledge the Atmospheric Toolbox®.

Conflicts of Interest: The authors declare no conflict of interest.

Appendix A

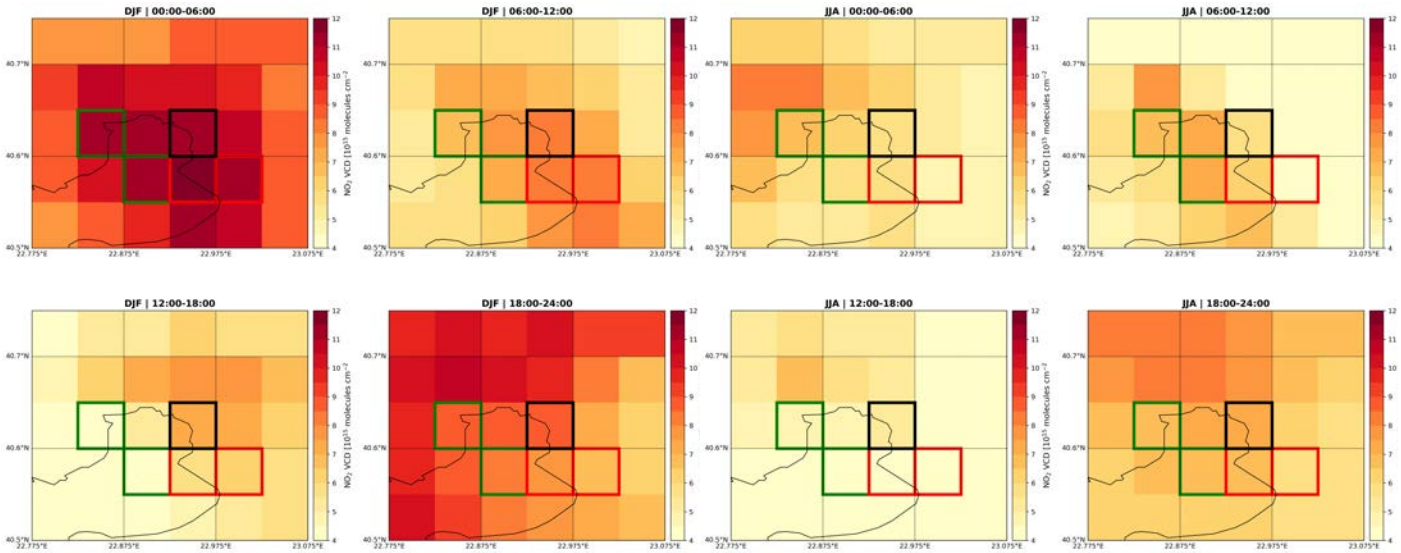

(a) **(b)**

Figure A1. LOTOS-EUROS tropospheric NO_2 columns (10^{15} molecules/cm^2) over Thessaloniki for (a) winter and (b) summertime, averaged within four 6h increments.

Preprints (www.preprints.org) | NOT PEER-REVIEWED | Posted: 27 April 2022 doi:10.20944/preprints202204.0257.v1

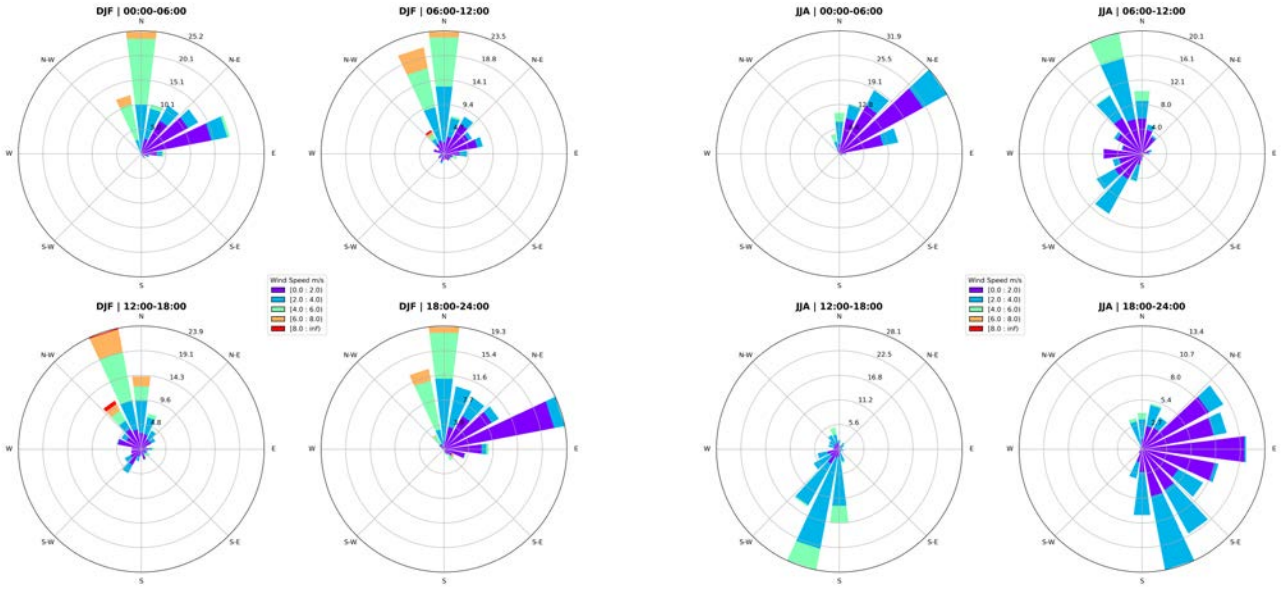

(a) **(b)**

Figure A2. Wind speed (ms^{-1}) and direction rose diagrams for the AUTH pixel for (a) winter and (b) summertime.

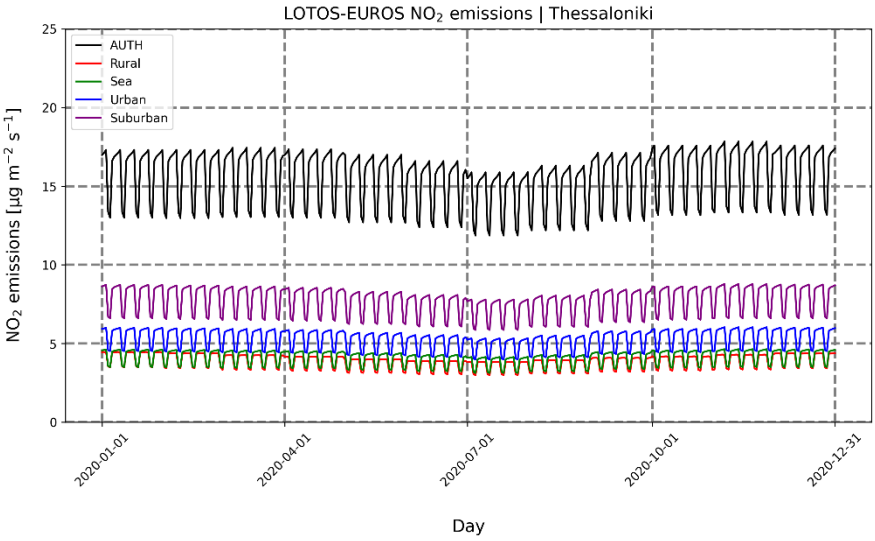

Figure A3. Weekly and seasonal variability of the NO_2 emissions ($\mu gm^{-2}s^{-1}$) over the specific locations around the urban area.

References

1. Akritidis D, Zanis P, Georgoulias AK, Papakosta E, Tzoumaka P, Kelessis A. Implications of COVID-19 Restriction Measures in Urban Air Quality of Thessaloniki, Greece: A Machine Learning Approach. *Atmosphere*. 2021; 12(11):1500. https://doi.org/10.3390/atmos12111500
2. Beirle, S., Platt, U., Wenig, M., and Wagner, T.: Weekly cycle of NO_2 by GOME measurements: a signature of anthropogenic sources, Atmos. Chem. Phys., 3, 2225–2232, https://doi.org/10.5194/acp-3-2225-2003, 2003.
3. Blechschmidt, A.-M., Arteta, J., Coman, A., Curier, L., Eskes, H., Foret, G., Gielen, C., Hendrick, F., Marécal, V., Meleux, F., Parmentier, J., Peters, E., Pinardi, G., Piters, A. J. M., Plu, M., Richter, A., Segers, A., Sofiev, M., Valdebenito, Á. M., Van Roozendael, M., Vira, J., Vlemmix, T., and Burrows, J. P.: Comparison of tropospheric NO_2 columns from MAX-DOAS retrievals and regional air quality model simulations, Atmos. Chem. Phys., 20, 2795–2823, https://doi.org/10.5194/acp-20-2795-2020, 2020.
4. Chan, K. L., Wiegner, M., van Geffen, J., De Smedt, I., Alberti, C., Cheng, Z., Ye, S., and Wenig, M.: MAX-DOAS measurements of tropospheric NO2 and HCHO in Munich and the comparison to OMI and TROPOMI satellite observations, Atmos. Meas. Tech., 13, 4499–4520, https://doi.org/10.5194/amt13-4499-2020, 2020
5. Drosoglou, T., Bais, A. F., Zyrichidou, I., Kouremeti, N., Poupkou, A., Liora, N., Giannaros, C., Koukouli, M. E., Balis, D., and Melas, D.: Comparisons of ground-based tropospheric NO2 MAX-DOAS measurements to satellite observations with the aid of an air quality model over the Thessaloniki area, Greece, Atmos. Chem. Phys., 17, 5829–5849, https://doi.org/10.5194/acp17-5829-2017, 2017.
6. Drosoglou, T., Koukouli, M. E., Kouremeti, N., Bais, A. F., Zyrichidou, I., Balis, D., van der A, R. J., Xu, J., and Li, A.: MAXDOAS NO_2 observations over Guangzhou, China; ground-based and satellite comparisons, Atmos. Meas. Tech., 11, 2239–2255, https://doi.org/10.5194/amt-11-2239-2018, 2018.
7. ESA: Copernicus Open Access Hub, available at: https://scihub.copernicus.eu/ (last access: 12 March 2022)
8. European Environmental Agency, EEA, Air Quality Data Service, 2022, available at: https://www.eea.europa.eu/ds_resolveuid/DAS-19-en, last access: 11.04.2022.
9. European Environmental Agency, EEA: Air quality in Europe – 2018 report, doi: 10.2800/777411, Luxembourg: Publications Office of the European Union, 2020, ISBN 978-92-9213-989-6, ISSN 1977-8449, available at: https://www.eea.europa.eu/publications/air-quality-in-europe-2018, last access: 18.11.2021.
10. European Environmental Agency, EEA: Air quality in Europe – 2020 report, doi:10.2800/786656, Luxembourg: Publications Office of the European Union, 2020, ISBN 978-92-9480-292-7, ISSN 1977-8449, available at: https://www.eea.europa.eu/publications/air-quality-in-europe-2020-report, last access: 18.11.2021.
11. European Union, EU: The Environmental Implementation Review 2019, COUNTRY REPORT: GREECE, available at https://ec.europa.eu/environment/eir/pdf/report_el_en.pdf , last access: 18.11.2021.
12. Fameli, K.M. and V.D. Assimakopoulos, Development of a road transport emission inventory for Greece and the Greater Athens Area: Effects of important parameters, Science of The Total Environment, 505, 2015, 770-786, https://doi.org/10.1016/j.scitotenv.2014.10.015.
13. Fountoukis, C. and Nenes, A.: ISORROPIA II: a computationally efficient thermodynamic equilibrium model for K^+–Ca^{2+}–Mg^{2+}–NH_4^+–Na^+–SO_4^{2-}–NO_3^-–Cl^-–H_2O aerosols, Atmos. Chem. Phys., 7, 4639–4659, https://doi.org/10.5194/acp-7-4639-2007, 2007.
14. Friedrich, M. M., Rivera, C., Stremme, W., Ojeda, Z., Arellano, J., Bezanilla, A., García-Reynoso, J. A., and Grutter, M.: NO2 vertical profiles and column densities from MAX-DOAS measurements in Mexico City, Atmos. Meas. Tech., 12, 2545–2565, https://doi.org/10.5194/amt-12-2545-2019, 2019.
15. Gery, M. W., Whitten, G. Z., Killus, J. P., and Dodge, M. C. (1989), A photochemical kinetics mechanism for urban and regional scale computer modeling, *J. Geophys. Res.*, 94(D10), 12925– 12956, doi:10.1029/JD094iD10p12925.
16. Gkertsi, F., Bais, A., Kouremeti, N., Drosoglou, T., Fountoulakis, I., and Fragkos, K.: DOAS-based total column ozone retrieval from Phaethon system, Atmos. Environ., 180, 51–58, https://doi.org/10.1016/j.atmosenv.2018.02.036, 2018
17. Guevara, M., Jorba, O., Tena, C., Denier van der Gon, H., Kuenen, J., Elguindi, N., Darras, S., Granier, C., and Pérez García-Pando, C.: Copernicus Atmosphere Monitoring Service TEMPOral profiles (CAMS-TEMPO): global and European emission temporal profile maps for atmospheric chemistry modelling, Earth Syst. Sci. Data, 13, 367–404, https://doi.org/10.5194/essd-13-367-2021, 2021.
18. Hönninger, G., von Friedeburg, C., and Platt, U.: Multi axis differential optical absorption spectroscopy (MAX-DOAS), Atmos. Chem. Phys., 4, 231–254, https://doi.org/10.5194/acp-4-231-2004, 2004.
19. Ialongo, I., Virta, H., Eskes, H., Hovila, J., and Douros, J.: Comparison of TROPOMI/Sentinel-5 Precursor NO_2 observations with ground-based measurements in Helsinki, Atmos. Meas. Tech., 13, 205–218, https://doi.org/10.5194/amt-13-205-2020, 2020.
in Greater Thessaloniki Area and the emission reductions needed for attaining the EU air quality legislation. Sci. Total Environ, https:// doi.org/10.1016/j.scitotenv.2008.10.034, 2009.
20. Karagkiozidis, D., Friedrich, M. M., Beirle, S., Bais, A., Hendrick, F., Voudouri, K. A., Fountoulakis, I., Karanikolas, A., Tzoumaka, P., Van Roozendael, M., Balis, D., and Wagner, T.: Retrieval of tropospheric aerosol, NO_2, and HCHO vertical profiles from MAX-DOAS observations over Thessaloniki, Greece: intercomparison and validation of two inversion algorithms, Atmos. Meas. Tech., 15, 1269–1301, https://doi.org/10.5194/amt-15-1269-2022, 2022.

21. Koukouli, M.E.; Skoulidou, I.; Karavias, A.; Parcharidis, I.; Balis, D.; Manders, A.; Segers, A.; Eskes, H.; Van Geffen, J. Sudden changes in nitrogen dioxide emissions over Greece due to lockdown after the outbreak of COVID-19. *Atmos. Chem. Phys.* 2021, *21*, 1759–1774, doi:10.5194/acp-21-1759-2021.
22. Kuenen, J. J. P., Visschedijk, A. J. H., Jozwicka, M., and Denier van der Gon, H. A. C.: TNO-MACC_II emission inventory; a multi-year (2003–2009) consistent high-resolution European emission inventory for air quality modelling, Atmos. Chem. Phys., 14, 10963–10976, https://doi.org/10.5194/acp-14-10963-2014, 2014.
23. Kuenen, J., Dellaert, S., Visschedijk, A., Jalkanen, J.-P., Super, I., and Denier van der Gon, H.: CAMS-REG-v4: a state-of-the-art high-resolution European emission inventory for air quality modelling, Earth Syst. Sci. Data, 14, 491–515, https://doi.org/10.5194/essd-14-491-2022, 2022.
24. Liora, N., Poupkou, A., Kontos, S. et al. Estimating Road Transport Pollutant Emissions Under Traffic-Congested Conditions with an Integrated Modelling Tool—Emissions Reduction Scenarios Analysis. Emiss. Control Sci. Technol. 7, 137–152 (2021). https://doi.org/10.1007/s40825-021-00191-5
25. Lopez-Restrepo, S.; Yarce, A., Pinel, N.; Quintero, O.L.; Segers, A., Heemink, A.W. Urban Air Quality, Modeling Using Low-Cost Sensor Network and Data Assimilation in the Aburrá Valley, Colombia. Atmosphere 2021, 12, https://doi.org/ 10.3390/atmos12010091
26. Manders, A. M. M., Builtjes, P. J. H., Curier, L., Denier van der Gon, H. A. C., Hendriks, C., Jonkers, S., Kranenburg, R., Kuenen, J. J. P., Segers, A. J., Timmermans, R. M. A., Visschedijk, A. J. H., Wichink Kruit, R. J., van Pul, W. A. J., Sauter, F. J., van der Swaluw, E., Swart, D. P. J., Douros, J., Eskes, H., van Meijgaard, E., van Ulft, B., van Velthoven, P., Banzhaf, S., Mues, A. C., Stern, R., Fu, G., Lu, S., Heemink, A., van Velzen, N., and Schaap, M.: Curriculum vitae of the LOTOS–EUROS (v2.0) chemistry transport model, Geosci. Model Dev., 10, 4145–4173, https://doi.org/10.5194/gmd-10-4145-2017, 2017.
27. Moussiopoulos, N., S. Papalexiou, P. Sahm, Wind flow and photochemical air pollution in Thessaloniki, Greece. Part I: Simulations with the European Zooming Model, Environmental Modelling & Software, Volume 21, Issue 12, 2006, Pages 1741-1751, ISSN 1364-8152, https://doi.org/10.1016/j.envsoft.2005.09.003.
28. Moussiopoulos, N, Vlachokostas, Ch., Tsilingiridis, G., Douros, I., Hourdakis, E., Naneris, C., Sidiropoulos, C.: Air quality status
29. Novak, J. H. and Pierce, T. E.: Natural emissions of oxidant precursors, Water Air Soil Poll., 67, 57–77, https://doi.org/10.1007/BF00480814, 1993.
30. Pinardi, G., Van Roozendael, M., Abuhassan, N., Adams, C., Cede, A., Clémer, K., Fayt, C., Frieß, U., Gil, M., Herman, J., Hermans, C., Hendrick, F., Irie, H., Merlaud, A., Navarro Comas, M., Peters, E., Piters, A. J. M., Puentedura, O., Richter, A., Schönhardt, A., Shaiganfar, R., Spinei, E., Strong, K., Takashima, H., Vrekoussis, M., Wagner, T., Wittrock, F., and Yilmaz, S.: MAX-DOAS formaldehyde slant column measurements during CINDI: intercomparison and analysis improvement, Atmos. Meas. Tech., 6, 167–185, https://doi.org/10.5194/amt-6-167-2013, 2013.
31. Platt, U. and Stutz, J.: Differential Optical Absorption Spectroscopy, Springer-Verlag Berlin Heidelberg, https://doi.org/10.1007/978-3-540-75776-4, 2008
32. Poupkou, A., Nastos, P., Melas, D., & Zerefos, C. (2011). Climatology of discomfort index and air quality index in a large urban Mediterranean agglomeration. *Water, Air, and Soil Pollution*, *222*(1–4), 163–183. https://doi.org/10.1007/s11270-011-0814-9
33. S5P MPC Routine Operations Consolidated Validation Report (ROCVR), Quarterly Validation Report of the Copernicus Sentinel-5 Precursor Operational Data Products #13: April 2018 – December 2021, S5P-MPC-IASB-ROCVR-13.01.00-20211217, https://s5p-mpc-vdaf.aeronomie.be/ProjectDir/reports//pdf/S5P-MPC-IASB-ROCVR-13.00.10-20211217_signed.pdf, edts: J.-C. Lambert and A. Keppens, issue number: version 06.0.1, 2021-12-17.
34. Schaub, D., Brunner, D., Boersma, K. F., Keller, J., Folini, D., Buchmann, B., Berresheim, H., and Staehelin, J.: SCIAMACHY tropospheric NO_2 over Switzerland: estimates of NOx lifetimes and impact of the complex Alpine topography on the retrieval, Atmos. Chem. Phys., 7, 5971–5987, https://doi.org/10.5194/acp-7-5971-2007, 2007.
35. Seinfeld, J. H. and S. N. Pandis, Atmospheric Chemistry and Physics: From Air Pollution to Climate Change, 3rd Edition, ISBN: 978-1-118-94740-1, New Jersey, John Wiley & Sons, Inc.
36. Sindosi, O. A., Georgios Markozannes, Evangelos Rizos & Evangelia Ntzani (2019) Effects of economic crisis on air quality in Ioannina, Greece, Journal of Environmental Science and Health, Part A, 54:8, 768-781, DOI: 10.1080/10934529.2019.1592534
37. Skoulidou, I., Koukouli, M.-E., Manders, A., Segers, A., Karagkiozidis, D., Gratsea, M., Balis, D., Bais, A., Gerasopoulos, E., Stavrakou, T., van Geffen, J., Eskes, H., and Richter, A.: Evaluation of the LOTOS-EUROS NO_2 simulations using ground-based measurements and S5P/TROPOMI observations over Greece, Atmos. Chem. Phys., 21, 5269–5288, https://doi.org/10.5194/acp-21-5269-2021, 2021.
38. Stavrakou, T., Müller, JF., Bauwens, M. et al. Satellite evidence for changes in the NO_2 weekly cycle over large cities. Sci Rep 10, 10066 (2020). https://doi.org/10.1038/s41598-020-66891-0
39. Stavroulas I, Grivas G, Michalopoulos P, Liakakou E, Bougiatioti A, Kalkavouras P, Fameli KM, Hatzianastassiou N, Mihalopoulos N, Gerasopoulos E. Field Evaluation of Low-Cost PM Sensors (Purple Air PA-II) Under Variable Urban Air Quality Conditions, in Greece. Atmosphere. 2020; 11(9):926. https://doi.org/10.3390/atmos11090926
40. van Geffen, J. H. G. M., Eskes, H. J., Boersma, K. F., Maasakkers J. D. and Veefkind, J. P., TROPOMI ATBD of the total and tropospheric NO_2 data products, Report S5P-KNMI-L2-0005-RP, version 1.4.0, released 6 Feb. 2019, KNMI, De Bilt, The Netherlands, available at http://www.tropomi.eu/documents/atbd/, last access: 08 May 2020.

41. Veefkind, J. P. et al. TROPOMI on the ESA Sentinel-5 Precursor: A GMES mission for global observations of the atmospheric composition for climate, air quality and ozone layer applications. Rem. Sens. Env. 120, 70–83 (2012), https://doi.org/10.1016/j.rse.2011.09.027.
Volume 268, 2022, 118809, ISSN 1352-2310, https://doi.org/10.1016/j.atmosenv.2021.118809.
42. Wang, H., Fang-Ying Gong, Sally Newman, Zhao-Cheng Zeng, Consistent weekly cycles of atmospheric NO_2, CO, and CO_2 in a North American megacity from ground-based, mountaintop, and satellite measurements, Atmospheric Environment, https://doi.org/10.1016/j.atmosenv.2021.118809, 2022.
43. Wang, Y., Lampel, J., Xie, P., Beirle, S., Li, A., Wu, D., and Wagner, T.: Ground-based MAX-DOAS observations of tropospheric aerosols, NO_2, SO_2 and HCHO in Wuxi, China, from 2011 to 2014, Atmos. Chem. Phys., 17, 2189–2215, https://doi.org/10.5194/acp-17-2189-2017, 2017.
44. World Health Organization, WHO: Ambient air pollution: A global assessment of exposure and burden of disease, World Health Organization, https://apps.who.int/iris/handle/10665/250141, ISBN: 9789241511353, Bonn, 2016, las access: 27.08.2021.